Development of a tapping device: a new needle insertion method for prostate brachytherapy

2006 Phys. Med. Biol. 51 891

(http://iopscience.iop.org/0031-9155/51/4/009)

Phys. Med. Biol. **51** (2006) 891–902 doi:10.1088/0031-9155/51/4/009

Development of a tapping device: a new needle insertion method for prostate brachytherapy

V Lagerburg, M A Moerland, M K Konings, R E van de Vosse, J J W Lagendijk and J J Battermann

Department of Radiotherapy, University Medical Center Utrecht, Heidelberglaan 100, 3584 CX Utrecht, The Netherlands

E-mail: v.lagerburg@azu.nl

Received 7 October 2005, in final form 11 November 2005
Published 25 January 2006
Online at stacks.iop.org/PMB/51/891

Abstract

The purpose of this study is to develop and test a tapping device for needle insertion for prostate brachytherapy. This device will tap the needle into the prostate with a certain, well-defined, amount of momentum, instead of the currently used method of pushing the needle. Because of the high needle insertion velocity, we expect prostate motion and deformation to be less compared to current methods. We measured the momentum that is applied when manually tapping the needle into the prostate and found a mean momentum of 0.50 ± 0.07 N s. The tapping device is pneumatically driven and we found that the delivered momentum increased linearly with the applied air pressure. The efficacy of the tapping device was tested on a piece of beef, placed on a freely moving and rotating platform. A significant correlation was found between the applied pressure and the rotation and displacement of the beef. Displacements and rotations were minimal for the highest pressure (4 bar) and amounted to only 2 mm and 6°, respectively. Higher air pressures will further reduce displacements and rotations.

(Some figures in this article are in colour only in the electronic version)

1. Introduction

Brachytherapy is one of the treatment possibilities for early stage prostate cancer. With brachytherapy, it is possible to deliver an adequate radiation dose to the prostate while sparing critical structures like the urethra, the neurovascular bundles, and the rectum (Merrick *et al* 2001, 2003a, 2003b, Stone and Stock 2002). One of the limiting factors of dose optimization in prostate brachytherapy is source placement precision. Seed positions that deviate from the pre-planned positions may influence the dose distribution in the prostate significantly (Dawson *et al* 1994, Moerland *et al* 1997).

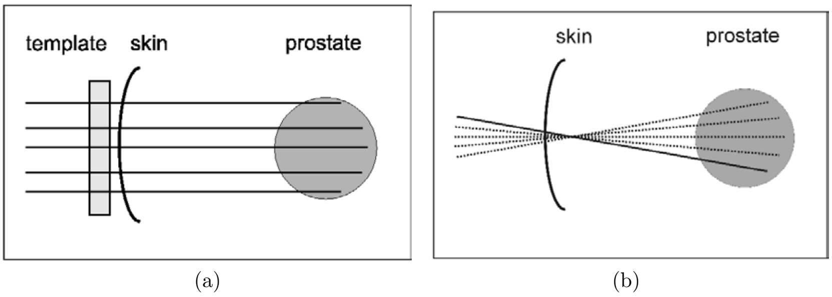

Figure 1. Schematic visualization of (a) the multi parallel needle method and (b) the single needle method.

The insertion of needles for prostate brachytherapy is currently done under ultrasound guidance (Holm *et al* 1983). Disadvantages of ultrasound-guided brachytherapy are the poor visibility of the prostate, especially at the base plane and the apex, which makes it difficult to estimate the prostate volume, and the difficulty of visualizing the implanted iodine seeds; hence intra-operative dose calculation is based on needle positions rather than seeds positions (Van Gellekom *et al* 2004).

Compared with ultrasound, magnetic resonance imaging (MRI) offers a better soft tissue contrast, which gives it the potential for better delineation of the prostate capsule and for definition of structures inside the prostate (Cheng and Tempany 1998, Husband *et al* 1998, Rasch *et al* 1999). This makes it possible to further optimize the dose distribution, for example by dose reduction in the penile bulb to reduce the risk of impotence (Merrick *et al* 2002) or by dose increase to the intraprostatic lesion to improve biochemical, disease-free survival (De Meerleer *et al* 2005).

Because of the limited space inside a closed bore MR scanner and the risk of pubic arch interference, current template guided transperineal implant techniques have their limitations (Ménard *et al* 2004, Susil *et al* 2004). The development of a single needle implant device, which can be placed between the legs of a patient in an MR scanner, can overcome these problems (Van Gellekom *et al* 2004). This robotic system will insert one needle from different angles into the prostate to deliver the seeds. After delivering the seeds, the needle will be retracted to the rotation point just beneath the skin and the insertion angle can be changed. The procedure will be performed without the use of a template or locking needles (figures 1(a) and (b)). With this method, it is not necessary to move the patient in and out the MR scanner during the procedure, as with other MR-guided prostate intervention methods (Ménard *et al* 2004, Susil *et al* 2004).

The single needle implant method is a needle-by-needle method, whereas in the current template guided method firstly all needles are placed before seed delivery. This means that, except for the first few needles, the prostate is fixed. Using the single needle method, the prostate can rotate with every new insertion of the needle.

Feygelman *et al* (1996) and Dattoli and Waller (1997) suggest that locking needles can help stabilize the prostate to reduce seed misplacement, while Taschereau *et al* (2000) found no effect of locking needles. Even if locking needles reduce the prostate motion, it is necessary to be able to predict the changes in prostate position and shape to be able to deliver the seeds at the desired position.

In our own study (Lagerburg *et al* 2005) we found that only rotation in the coronal plane can be more or less predicted and reduced by the use of locking needles. Rotation in the sagittal plane cannot be predicted nor reduced by the use of locking needles. The maximum rotation we found in the coronal plane was 13.8° without locking needles and 7.8° with locking needles. In the sagittal plane, the maximum rotation was 8.5° without locking needles and 10.2° with locking needles. The rotation of the prostate results in a deviation between the real seed position and the planned seed position. With a prostate rotation of 13.8° and a strand existing of four seeds, the maximum displacement of the seeds relative to the planned position that can occur is 8.4 mm

Prostate motion (rotation and displacement) and needle divergence are known causes of source misplacement (Roberson *et al* 1997, Nath *et al* 2000). Needles for prostate brachytherapy are currently pushed into the prostate by the physician. Due to the elastic properties of the prostate this results in movement and deformation of the prostate. This makes it difficult to deliver the seeds to the desired (pre-planned) position.

In this study, we introduce a new needle insertion method to decrease prostate movement and deformation. Instead of pushing, the needle is tapped into the prostate. Due to the high needle insertion velocity, we expect the prostate to move less. We have made a device for needle insertion with a controlled velocity. The device will give a certain, well-defined, amount of momentum to the needle. With every tap the needle will be inserted at most a certain, pre-defined, distance (for example 5 mm) into the prostate. This tapping device is the first part of the single needle implant device (SNID) (Van Gellekom *et al* 2004), which will be developed at our department and used for MRI-guided brachytherapy.

Apart from prostate brachytherapy, this new needle insertion method can also be useful for other applications where tissue movement due to needle insertion is problematic, such as breast biopsies (Deurloo *et al* 2001).

The purpose of this study is to measure the momentum that is necessary to insert a needle into the prostate and to develop and test a device that taps a needle into the prostate with a certain, well-defined, amount of momentum.

2. Methods and materials

To develop a device that taps a needle into the prostate, it is necessary to know the minimum momentum that is needed to insert a needle into the prostate. This momentum was measured during the normal procedure for prostate brachytherapy. The needle was tapped into the prostate by a physician (JJB). The momentum was measured with a Flexiforce A201 sensor from Tekscan. The momentum that can be delivered by the tapping device is adjustable by changing the air pressure of the pneumatic cylinder. The working of the tapping device was tested on a piece of beef. Beef displacement and rotation were measured for different air pressures.

2.1. Calibration of the flexiforce sensor

The Flexiforce A201 sensor is a flexible, thin film force sensor. The application of force to the sensor results in a change of the resistance of the sensing element, which is inversely proportional to the force applied. The sensor is suitable for measuring both static and dynamic forces. The sensor has to be calibrated to be able to convert the output into the appropriate engineering units.

The experimental set-up to calibrate the Flexiforce sensor consisted of a pendulum and a hammer (see figure 2). The Flexiforce sensor was attached to the pendulum and the hammer was used to create a momentum p. The principle of the experimental set-up is based on the law of conservation of angular momentum for a completely inelastic collision (equation (1)),

$$R_{\text{impact}} m_h v_h = L_{\text{tot,before}} = L_{\text{tot,after}} = I_p \omega_p \tag{1}$$

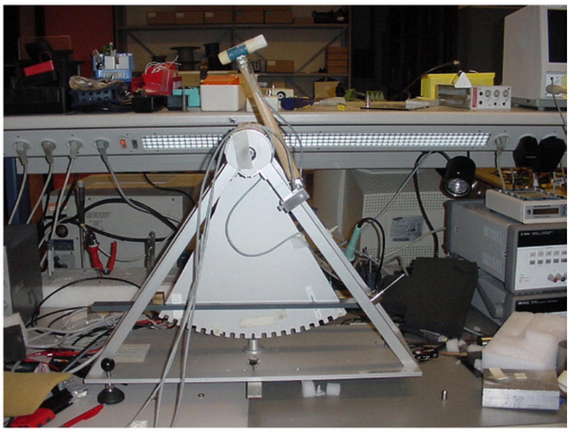

Figure 2. Experimental set-up for the calibration of the Flexiforce sensor.

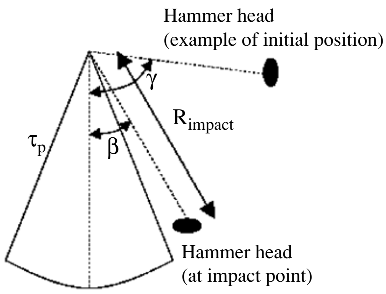

Figure 3. Schematic overview of the experimental calibration set-up.

where R_{impact} is the arm of the momentum (see also figure 3), m_h is the mass of the hammer, v_h is the velocity of the hammer immediately before impact, $L_{\text{tot,before}}$ is the total angular momentum before the impact, $L_{\text{tot,after}}$ is the total angular momentum after impact, I_p is the moment of inertia of the combination of the pendulum and the hammer, and ω_p is the angular velocity of the pendulum.

The hammer is released from a certain height. Depending on this height, the hammer will have a certain velocity before it hits the Flexiforce sensor attached to the pendulum. Then the pendulum will start moving. The initial position of the hammer, the starting angle γ, was different for every measurement and the value of the Flexiforce sensor F_{flex} and the maximum angular velocity ω of the pendulum were measured. With these values and equations (3) and (4) it was possible to calibrate the sensor. With this experimental set-up, there were two possibilities to calibrate the sensor, namely, with the starting angle of the hammer (equation (4)) and with the angular velocity of the pendulum after impact (equation (3)). Both should give the same value for the conversion between the output of the Flexiforce sensor and the force.

The relationship between force and momentum is as follows:

$$\int_0^t F\,\mathrm{d}t = mv = p. \tag{2}$$

The value of the Flexiforce sensor is related to the angular velocity of the pendulum by

$$\int_0^{\tau} F_{\text{flex}}\, \mathrm{d}t = \frac{I_p \omega_p c}{R_{\text{impact}}} = \frac{m_p c r_p^2 \omega_p}{4R_{\text{impact}}} \tag{3}$$

where τ is the time duration of the impact process, F_{flex} is the output of the Flexiforce sensor, c is the conversion value between the output of the Flexiforce sensor and the force, and r_p is the radius of the pendulum.

The value of the Flexiforce sensor is related to the starting angle of the hammer by

$$\int_0^{\tau} F_{\text{flex}}\, \mathrm{d}t = m_h c \sqrt{2 g h_h (\cos(\beta) - \cos(\gamma))} \tag{4}$$

where g is the acceleration of gravity, h_h is the distance of the centre of mass with respect to the point of rotation of the hammer and β is the angle where the hammer hits the Flexiforce sensor (see also figure 3).

2.2. Momentum measurements

The momentum measurements were performed during the procedure for prostate brachytherapy. The patient was placed in the lithomy position and a Foley catheter was placed *in situ*. A rectangular template with 5 mm spaced holes is positioned against the perineum. For our study, the normal procedure was changed slightly for the first few inserted needles. Instead of pushing the needle into the prostate, the physician tapped the needle (18G) into the prostate using the same hammer that was used for the calibration measurements. The Flexiforce sensor was attached to the end of the needle. The output from the Flexiforce sensor was recorded after each tap, using an oscilloscope, and then transferred to a laptop. During the procedure, the real-time ultrasound images of the prostate were recorded on video, on which we measured the distance that the needle was inserted into the prostate with every tap. This was measured because we expected a correlation between the used momentum and the distance that the needle was inserted into the prostate. The momentum measurements were performed in two patients. In total the insertion of six needles was analysed. After the insertion of the first few needles the normal procedure went on.

2.3. The tapping device

Figure 4 shows a schematic overview of the tapping device. The pneumatic cylinder used is a Festo ADVULQ-25-40-A-P-A-S20 (Delft, The Netherlands), with a maximum stroke of 40 mm. The pneumatic cylinder moves forward while pushing a sliding load. After the pneumatic cylinder reaches its maximum stroke the sliding load moves further with a constant velocity and hits the needle. The maximum insertion depth of the needle per tap is adjustable and a buffer stop is built in to prevent the insertion depth to exceed the previously defined distance. The maximum velocity of the pneumatic cylinder and thus the needle insertion velocity are adjustable by changing the air pressure.

The Flexiforce sensor was used to measure the momentum of the tapping device with different pressures (1 to 4 bar) and with two different sliding loads (33.2 g and 121.6 g). The tapping device should be able to deliver at least the same amount of momentum to the needle as the physician needed to insert a needle into the prostate.

The working of the tapping device was tested on a piece of beef. The beef was placed on a free rotating and movable platform (see figure 5). The rotation (in the coronal plane) and translation (in the cranio-caudal direction) of the beef were measured for air pressures

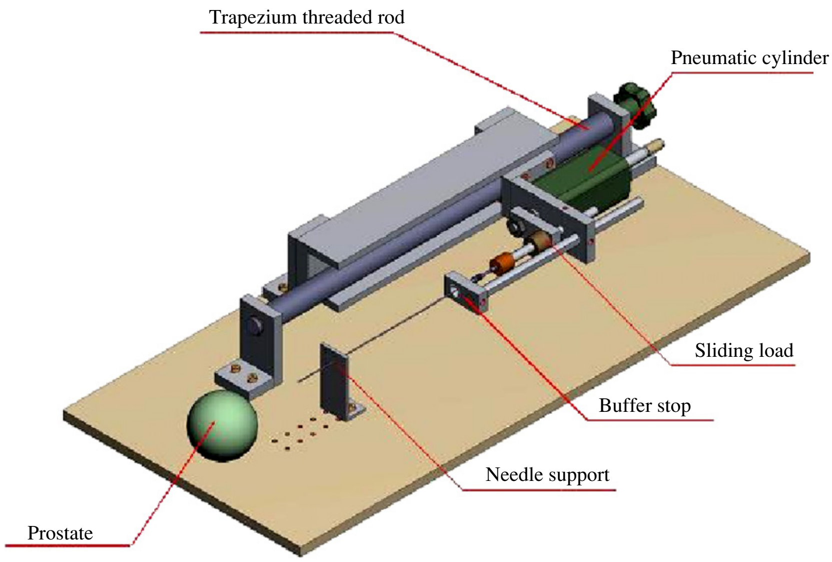

Figure 4. Schematic overview of the tapping device.

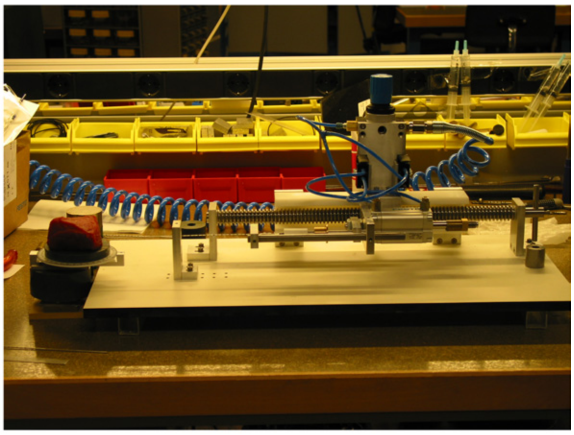

Figure 5. Experimental set-up of the tapping device and the beef.

between 1 and 4 bar, after the needle was inserted 3, 4, 5 and 6 cm into the beef. The needle was inserted in the middle, 1 cm to the left and right, and 2 cm to the left and right of the beef.

3. Results

The calibration measurements were used to relate the values of the Flexiforce sensor, found during the brachytherapy experiments and during the experiments with the tapping device, to the force. There were two different conversion values found. With equation (3) a value for c of 107.4 ± 18 was found and with equation (4) a value for c of 73.2 ± 10.1 was found. There is a difference between these two values because after the collision the impulse from

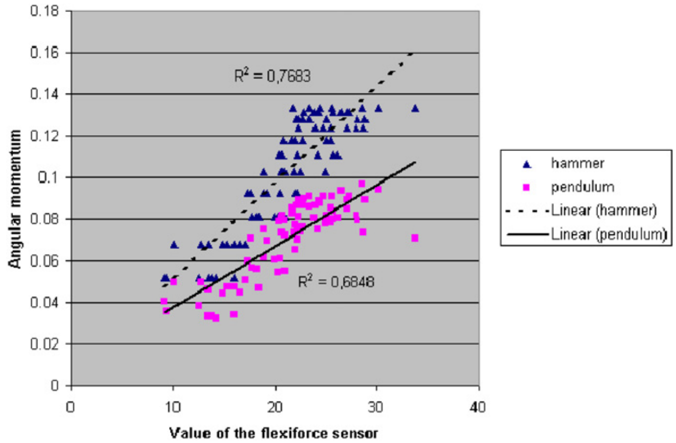

Figure 6. Relation between the value of the Flexiforce sensor and the angular momentum calculated with equation (3) for the pendulum and equation (4) for the hammer.

the hammer is not totally transferred to the pendulum. For this reason, we used the value of 73.2 ± 10.1 for our further calculations. In figure 6 an overview of the results is given.

During the brachytherapy procedure, a mean of 3.7 taps per needle was necessary to insert the needle into the prostate. The needle was inserted between 4.25 mm and 17.5 mm (mean 7.9 mm) into the prostate per tap. The momentum used to tap the needle into the prostate varied from 0.13 ± 0.02 N s to 1.16 ± 0.15 N s with a mean momentum of 0.50 ± 0.07 N s. For the first tap there was a significant correlation ($R = 0.912$, $p = 0.011$) between the momentum used and the distance that the needle was inserted into the prostate. There is also a significant correlation ($R = 0.620$, $p = 0.002$) between the distance that the needle is already inserted into the prostate and the momentum needed to further insert the needle into the prostate. This means that for the first tap the relation between the momentum used and the distance that the needle was inserted into the prostate is different than that for, for example, the third tap

$$\text{tap 1} : d = 0.29 \times c \times p \tag{5}$$

$$\text{tap 3} : d = 0.18 \times c \times p \tag{6}$$

where d is the distance (in mm) that the needle is inserted into the prostate per tap, c is the conversion value between the output of the Flexiforce sensor and the force, and p is the momentum (in N s) of the tap.

The momentum delivered by the tapping device depends on the used pressure and sliding load. The higher the pressure and the mass of the sliding load, the higher the achieved momentum. In figure 7 the results of the measurements with the Flexiforce sensor in the tapping device are shown for the heaviest sliding load. When the sliding load of 121.6 g and an air pressure of 4 bar are used the maximum momentum we can achieve is 0.37 ± 0.05 N s. The insertion velocity of the needle depends on its weight. The needle insertion velocity we could reach during the experiment with the beef was 31 m s^{-1}.

The working of the automatic tapping device was tested on a piece of beef. An overview of the displacements and rotations of the beef for the two different sliding loads and the different air pressures is given in table 1. It was shown that the displacement of the beef was significantly less for the most heavy load ($p = 0.002$). For the rotation there was no

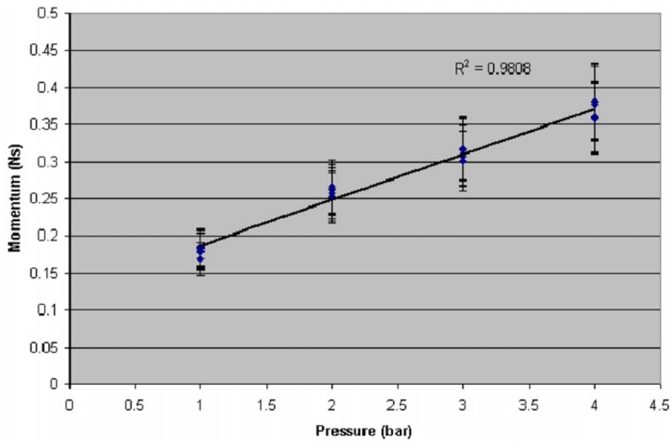

Figure 7. Relation between the air pressure and the momentum for the tapping device. The error bars give the standard deviation of the momentum.

Table 1. Minimum, maximum and mean rotations (absolute) and displacements of the beef for the two different sliding loads (33.1 g and 161.2 g) and different air pressures (1 to 4 bar). In the last column, the maximum insertion depth of the needle into the beef is mentioned.

Load	Pressure		Minimum	Maximum	Mean	In beef (maximum)
Light	1	Rotation (°)	2.0	6.0	3.6	4.1
		Displacement (mm)	4.0	14.0	10.4	
Light	2	Rotation	0.0	9.0	3.2	6.0
		Displacement	0.5	8.0	3.7	
Light	3	Rotation	0.0	6.5	1.9	6.3
		Displacement	1.0	6.0	2.8	
Light	4	Rotation	0.0	10.0	2.8	6.3
		Displacement	1.0	5.5	2.4	
Heavy	1	Rotation	0.0	16.0	4.3	5.7
		Displacement	0.0	10.0	4.3	
Heavy	2	Rotation	0.0	9.0	3.5	6.4
		Displacement	1.0	5.0	2.8	
Heavy	3	Rotation	1.0	6.0	3.3	6.2
		Displacement	0.0	4.0	1.5	
Heavy	4	Rotation	0.0	6.0	1.3	7.1
		Displacement	0.0	2.0	1.0	

significant difference found. Because we decided to use the most heavy load the rest of the results will be related to that load. A significant correlation of 0.753 ($p < 0.01$) was found between the rotation of the beef and the place of insertion of the needle. The correlation between the rotation and the pressure was -0.250 ($p = 0.037$). The displacement of the beef was correlated with the pressure and thus with the velocity of the pneumatic cylinder ($R = -0.717$; $p < 0.01$, see figure 8). There was no correlation found between the displacement of the beef and the place of insertion of the needle. The maximum displacement found with a pressure of 4 bar was 2 mm, and in all these cases the needle was inserted at least 4 cm into the beef. The maximum rotation found was 6°, and this was after the needle was inserted 5 cm into the beef.

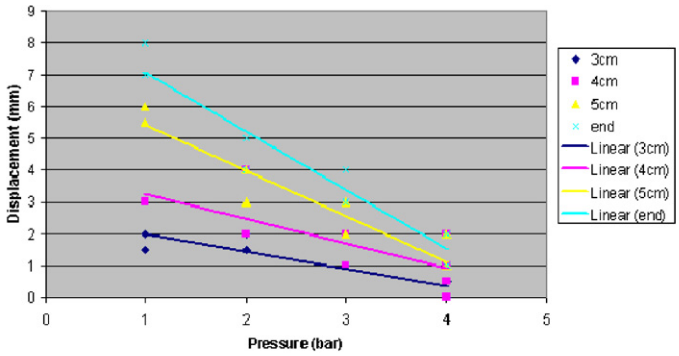

Figure 8. Relation between the air pressure and the displacement of the beef.

4. Conclusion and discussion

In this study, a new method of needle insertion for prostate brachytherapy is described, namely tapping the needle into the prostate instead of pushing. To be able to do this in a controlled and reproducible way, a tapping device was developed. Before making this device, the momentum needed to tap a needle into the prostate was measured during a normal brachytherapy procedure. The working of the tapping device was tested on a piece of beef.

Some research has already been done to measure or model the forces during needle insertion (Holton 2001, Kataoka *et al* 2002, Maurin *et al* 2004, Okamura *et al* 2004) and even a medical needle drive to investigate experimentally the mechanics of needle introduction in soft tissue already exists (Lefrançois and Sloboda 2003). In our research, we measured the momentum during needle insertion instead of the force. This is done because we made a device that taps a needle into the prostate with a high velocity and a certain, well-defined, amount of momentum, instead of the currently used method of pushing the needle. With this method, we expect the prostate motion to be less. Furthermore, using momentum instead of force is safe to use. When the needle encounters, for example, a bony structure it will only transfer its momentum to the bony structure in a collision. It will not penetrate the bone as would happen when the needle was pushed into the prostate. The tapping robot will need a feedback system to detect incomplete needle insertion due to obstructions so that tapping is stopped under such circumstances.

During the calibration of the Flexiforce sensor, we found two different constants for the conversion between the output of the sensor and the real force. The value we found with equation (3) for the pendulum was higher than the value we found with equation (4) for the hammer. This difference exists because the hammer does not transfer all its momentum to the pendulum after the collision, but it bounces back and continues moving. To prevent the hammer from bouncing back after the collision, we attached a needle to the flexiforce sensor and a piece of foam to the hammer, so the hammer will move together with the pendulum after the collision. With this method still not all the momentum from the hammer is transferred to the pendulum, but more than without the foam and the needle. The difference found between the momentum of the hammer and of the pendulum can be explained with a bouncing back of the hammer of 7° (mean value), which corresponds with our observations during the experiments. Because of the above-mentioned reason, we used the conversion value calculated with equation (4) for further calculations. The value from equation (3) was only used as a reference value.

The spread in the conversion value can be due to three things: the hammer will not always hit the pendulum in exactly the same way, which influences the value of the Flexiforce sensor; the movement of the hammer is not free of friction, which will also have its influence on the measurements; the sensor also has its own non-linearity.

During the brachytherapy experiments, a correlation was found between the distance that the needle is already inserted into the prostate and the momentum needed to further insert the needle into the prostate. This indicates that there is friction between the needle and the prostate tissue. The correlation between the momentum used and the distance that the needle is inserted into the prostate decreases for every tap. This is probably also due to the friction between the needle and the prostate tissue. Because the needles are not inserted the same distance for each tap the influence of the friction differs for every tap.

With the tapping device it is possible to insert a needle into the prostate with different velocities. Before starting the experiments, we expected the prostate motion to correlate with the needle insertion velocity. This expectation was supported by the simulation studies of Alterovitz and Goldberg (2003) where they found that seed placement errors decrease with higher needle insertion velocities. During the beef experiments, it was shown that this expectation is correct for the displacement and the rotation of the beef. The higher the velocity, the less displacement and rotation was found.

Displacement and deformation of the prostate during needle insertion were the subject of several theoretical and simulation studies (DiMaio and Salcudean 2002, Alterovitz *et al* 2003, Alterovitz and Goldberg 2003, DiMaio and Salcudean 2003), but measured data are scarce (Dattoli and Waller 1997, Stone *et al* 2002). Dattoli and Waller (1997) found a displacement of the prostate of 1 cm without locking needles and 0.2 mm with the use of locking needles in the lateral direction. Stone *et al* (2002) found the maximum movement of the prostate in the cranial-caudal direction that ranged from 0 to 30 mm (median 15 mm). In the lateral plane, a mean displacement of 1.93 and a maximum displacement of 4.61 mm was found. In the anterior–posterior plane, a mean displacement of 2.60 mm and a maximum displacement of 5.86 mm was found. In our experiments with the beef, we only tested for displacement along the cranio-caudal direction and a maximum displacement of 2 mm was found with an air pressure of 4 bar. This is significantly less than the displacement found in the literature.

To our knowledge, only a little is known about prostate rotation due to needle insertion. In our own study, we found that the maximum rotation in the coronal plane was 13.8° and in the sagittal plane 8.5° when no locking needles were used and the needles were pushed into the prostate (Lagerburg *et al* 2005). In our tapping experiments with the beef, the rotation was only measured in the coronal plane and a maximum rotation of 6° was found.

The next step in this study will be to test this device on patients to see whether the prostate movement and rotation really becomes less with this new needle insertion method. During these tests we also have to see if the momentum requires changes after several insertions due to a decrease in the sharpness of the needle.

In conclusion, an automatic tapping device was developed to insert a needle into the prostate for prostate brachytherapy. The experiments on beef showed that displacement and rotation due to tapping were less than found in the literature when a needle was pushed into the prostate. From the brachytherapy experiments, we can conclude that the optimal momentum of the tapping device may be somewhat higher than the currently used 0.37 N s, resulting in even less phantom movement.

Apart from prostate brachytherapy, this new needle insertion method can also be useful for other applications where tissue movement due to needle insertion is problematic, such as breast biopsies (Deurloo *et al* 2001).

References

Alterovitz R and Goldberg K 2003 Needle insertion and radioactive seed implantation in human tissues: simulation and sensitivity analysis *IEEE Int. Conf. on Robotics and Automation* pp 1793–99

Alterovitz R, Pouliot J, Taschereau R, Hsu I C J and Goldberg K 2003 Simulating needle insertion and radioactive seed implantation for prostate brachytherapy in *Medicine Meets Virtual Reality* pp 19–25

Cheng D and Tempany C M C 1998 MR imaging of the prostate and bladder *Seminars in US, CT, and MRI* **19** 67–89

Dattoli M and Waller K 1997 A simple method to stabilize the prostate during transperineal prostate brachytherapy *Int. J. Radiat. Oncol. Biol. Phys.* **38** 341–2

Dawson J E, Wu T, Roy T, Gu J Y and Kim H 1994 Dose effects of seeds placement deviations from pre-planned positions in ultrasound guided prostate implants *Radiother. Oncol.* **32** 268–70

De Meerleer G, Villeirs G, Bral S, Paelinck L, De Gersem W, Dekuyper P and De Neve W 2005 The magnetic resonance detected intraprostatic lesion in prostate cancer: planning and delivery of intensity-modulated radiotherapy *Radiother. Oncol.* **75** 325–33

Deurloo E E, Gilhuijs K G A, Schultze Kool L J and Muller S H 2001 Displacement of breast tissue and needle deviations during stereotactic procedures *Invest. Radiol.* **36** 347–53

DiMaio S P and Salcudean S E 2002 Needle insertion modelling for the interactive simulation of percutaneous procedures *Medical Image Computation and Computer-Assisted Intervention* pp 253–60

DiMaio S P and Salcudean S E 2003 Needle insertion modelling and simulation *IEEE Trans. Robot. Autom.* **19** 864–75 (special issue on Medical Robotics)

Feygelman V, Friedland J L, Sanders R M, Noriega B K and Pow-Sang J M 1996 Improvement in dosimetry of ultrasound-guided prostate implant with the use of multiple stabilization needles *Med. Dosim.* **21** 109–12

Holm H H, Juul N, Pedersen J F, Hansen H and Strøyer I 1983 Transperineal Iodine-125 seed implantation in prostatic cancer guided by transrectal ultrasonography *J. Urol.* **130** 283–6

Holton L L H 2001 Force models for needle insertion created from measured needle puncture data *Stud. Health Technol. Inform.* **81** 180–6

Husband J E, Padhani A R, Macvicar A D and Revell P 1998 Magnetic resonance imaging of prostate cancer: comparison of image quality using endorectal and pelvic phased array coils *Clin. Radiol.* **53** 673–81

Kataoka H, Washio T, Chinzei K, Mizuhara K, Simone C and Okamura A M 2002 Measurement of the tip and friction force acting on a needle during penetration *Proc. 5th Int. Conf. on Medical Image Computing and Computer Assisted Intervention* pp 216–23

Lagerburg V, Moerland M A, Lagendijk J J W and Battermann J J 2005 Measurement of prostate rotation during insertion of needles for brachytherapy *Radiother. Oncol.* **77** 318–23

Lefrançois R and Sloboda R S 2003 A medical needle drive for the study of interstitial implant mechanics *Med. Eng. Phys.* **25** 255–8

Maurin B, Barbe L, Bayle B, Zanne P, Gangloff J, De Mathelin M, Gangi A, Soler L and Forgione A 2004 In vivo study of forces during needle insertions *Proc. Medical Robotics, Navigation and Visualisation Scientific Workshop*

Ménard C *et al* 2004 MRI-guided HDR prostate brachytherapy in standard 1.5T scanner *Int. J. Radiat. Oncol. Biol. Phys.* **59** 1414–23

Merrick G S, Butler W M, Wallner K E, Galbreath R W and Lief J H 2003a Long-term urinary quality of life after permanent prostate brachytherapy *Int. J. Radiat. Oncol. Biol. Phys.* **56** 454–61

Merrick G S, Butler W M, Wallner K E, Hines A L and Allen Z 2003b Late rectal function after prostate brachytherapy *Int. J. Radiat. Oncol. Biol. Phys.* **57** 42–8

Merrick G S, Butler W M, Wallner K E, Lief J H, Anderson R L, Smeiles B J, Galbreath R W and Benson M L 2002 The importance of radiation doses to the penile bulb versus crura in the development of postbrachytherapy erectile dysfunction *Int. J. Radiat. Oncol. Biol. Phys.* **54** 1055–62

Merrick G S, Wallner K, Butler W M, Galbreath R W, Lief J H and Benson M L 2001 A comparison of radiation dose to the bulb of the penis in men with and without prostate brachytherapy-induced erectile dysfunction *Int. J. Radiat. Oncol. Biol. Phys.* **50** 597–604

Moerland M A, Wijrdeman H K, Beersma R, Bakker C J G and Battermann J J 1997 Evaluation of permanent I-125 prostate implants using radiography and magnetic resonance imaging *Int. J. Radiat. Oncol. Biol. Phys.* **37** 927–33

Nath S, Chen Z, Yue N, Trumpore S and Peschel R 2000 Dosimetric effects of needle divergence in prostate seed implant using I-125 and Pd-103 radioactive seeds *Med. Phys.* **27** 1058–66

Okamura A M, Simone C and O'Leary M D 2004 Force modeling for needle insertion into soft tissue *IEEE Trans. Biomed. Eng.* **51** 1707–16

Rasch C, Barillot I, Remeijer P, Touw A, Van Herk M and Lebesque J V 1999 Definition of the prostate in CT and MRI: a multi-observer study *Int. J. Radiat. Oncol. Biol. Phys.* **43** 57–66

Roberson P L, Narayana V, McShan D L, Winfield R J and McLaughlin P W 1997 Source placement error for permanent implant of the prostate *Med. Phys.* **24** 251–7

Stone N N, Roy J, Hong S, Lo Y C and Stock R G 2002 Prostate gland motion and deformation caused by needle placement during brachytherapy *Brachytherapy* **1** 154–60

Stone N N and Stock R G 2002 Complications following permanent prostate brachytherapy *Eur. Urol.* **41** 427–33

Susil R C, Camphausen K, Choyke P, McVeigh E R, Gustafson G S, Ning H, Miller R W, Atalar E, Coleman C N and Ménard C 2004 System for prostate brachytherapy and biopsy in a standard 1.5T MRI scanner *Magn. Reson. Med.* **52** 683–7

Taschereau R, Pouliot J, Roy J and Tremblay D 2000 Seed misplacement and stabilizing needles in transperineal permanent prostate implants *Radiother. Oncol.* **55** 59–63

Van Gellekom M P R, Moerland M A, Battermann J J and Lagendijk J J W 2004 MRI-guided prostate brachytherapy with single needle method-a planning study *Radiother. Oncol.* **71** 327–32